JOURNAL OF SPACECRAFT AND ROCKETS
Vol. 37, No. 6, November–December 2000

Optimization Methodology for Ascent Trajectories of Lifting-Body Reusable Launchers

Salvatore D'Angelo* and Edmondo Minisci†
Politecnico di Torino, 10129 Turin, Italy
Daniele Di Bona‡
FIAT Iveco S.p.A., 10156 Turin, Italy
and
Luciano Guerra§
Alenia Aerospazio S.p.A., 10146 Turin, Italy

A simulation and optimization methodology, created by the authors to optimize the trajectories of airbreathing spaceplanes and already tested and validated, has been improved and applied to a new concept of single-stage-to-orbit lifting-body spaceplane in order to search for optimal ascent trajectories for a typical mission profile. After a brief discussion on preliminary assumptions concerning the available data set, we first present the analysis procedure and the calculation method, which allowed us to simulate the ascent trajectory of a single-stage spaceplane model, able to connect the Earth-launch pad to the International Space Station. The optimization technique, belonging to the class of direct optimization methods and dealing with a wide number of independent parameters, is then described in detail, and specific results ensuring a better payload/liftoff weight ratio are widely shown. Shape and size of the vehicle as well as integrated propulsion system and weight distribution are derived from a complete data set, whereas the aerodynamic performances have been directly generated via a Navier–Stokes code. Finally, a sensitivity analysis by varying launch-pad location and final orbit inclination and altitude has been performed, and the influence of each guidance and control parameter on the optimal ascent trajectory has been emphasized.

Nomenclature

$\boldsymbol{A}$	=	total aerodynamic force, N
a	=	orbit major semi-axis, m
C_s	=	sound speed, m/s
D	=	aerodynamic drag force, N
F	=	boundary condition
G	=	generic path constraint
GM	=	Earth's gravitational parameter
$\boldsymbol{g}$	=	acceleration of gravity, m/s^2
g_0	=	sea-level acceleration of gravity (9.80665 m/s^2)
h	=	flight altitude above sea level, m
I_{sp}	=	specific impulse, s
i	=	orbit inclination, deg
L	=	aerodynamic lift force, N
M	=	Mach number
M_A	=	aerodynamic moment, N·m
M_P	=	propulsion moment, N·m
m	=	vehicle mass, kg
P	=	atmospheric pressure, Pa
$\boldsymbol{QO}$	=	vector joining Earth center to spacecraft position
R	=	Earth radius (6378 km)
$\boldsymbol{T}$	=	thrust, N
$\boldsymbol{V}$	=	air speed, m/s
$\boldsymbol{V}_i$	=	inertial velocity, m/s
V_{orb}	=	orbital velocity, m/s
X_{CG}	=	center of gravity position, m
α	=	angle of attack, deg
γ	=	velocity pitch (path inclination angle), deg
δ	=	power setting
δ_f	=	body-flap deflection, deg
ε	=	thrust angle, deg
θ	=	geographical longitude, deg
λ	=	geographical latitude, deg
μ	=	velocity roll (bank angle), deg
ρ	=	air density, kg/m^3
τ	=	differential power setting
χ	=	velocity yaw (path direction angle), deg
ω_e	=	Earth angular rate (7.2722e-5 rad/s)

Received 3 August 1999; presented as Paper 99-4165 at the Atmospheric Flight Mechanics Conference, Portland, OR, 9–11 August 1999; revision received 22 June 2000; accepted for publication 22 June 2000.

*Associate Professor, Department of Aerospace Engineering, Corso Duca degli Abruzzi 24. Member AIAA.
†Graduate Student, Department of Aerospace Engineering, Corso Duca degli Abruzzi 24.
‡Project Engineer, IVECO Process Engineering Center, Lungo Stura Lazio 49. Member AIAA.
§Senior Engineer, Corso Marche 41.

Introduction

THE present demand of reduction in both design and operational costs has oriented the aerospace community to research and develop new space launcher vehicles, where scientific and technological innovations are continuously introduced. To obtain the same performances of present multistage expendable launch vehicles, an equivalent single-stage spaceplane should include a total propellant weight up to 90% of the liftoff mass. Moreover, it should be also powered by an efficient propulsion system able to operate at each flight condition during the whole ascent trajectory, from takeoff at sea level to insertion into the final orbit.

During the last years several fully reusable single-stage-to-orbit (SSTO) concepts, powered by fully rocket propulsion systems (like Venture-Star), have been investigated to obtain a vehicle able to connect more frequently the Earth ground pad with the International Space Station (ISS). Under this scenario the definition of optimal ascent trajectories has revealed great advantages in order to ensure the better payload to liftoff weight ratio of SSTO reusable launchers.

The main goal of this paper, which reflects the main contribution to the field, is to provide a simulation and optimization methodology able to investigate different ascent trajectories of a SSTO lifting-body vehicle, according to several mission profiles. Nevertheless, the concept vehicle adopted in this study is not merely a case example to illustrate the methodology, but the obtained results in terms of final payload carried on orbit are as realistic as the aerodynamic, propulsive, and weight distribution models are validated. Starting from the equation of motion, the original optimization code,

which was successful for trajectories optimization of SSTO vehicles in airbreathing configuration,[1] has been implemented with new further routines able to obtain rapidly a suitable set of parameters for the optimal starting conditions (good starting point) and to define better the strategy to reach the minimum of the objective function (multistep strategy).

Mathematical Model

The equations of motion describing the flight of a spacecraft reaching orbital speed over a spherical rotating Earth are derived with the assumptions that the trajectory is flown in the immediate neighborhood of the Earth, and the differential effects of the sun and the moon on the motion of the Earth-vehicle system are neglected.[2] Because of the these hypotheses, the vectorial dynamical equation can be written in the following form:

$$\boldsymbol{T} + \boldsymbol{A} + m\boldsymbol{g} = \left[\frac{\mathrm{d}\boldsymbol{V}}{\mathrm{d}\boldsymbol{t}} + 2\boldsymbol{\omega}_e \times \boldsymbol{V} + \boldsymbol{\omega}_e \times (\boldsymbol{\omega}_e \times \boldsymbol{QO}) \right] \quad (1)$$

where the inertia terms represent the relative, Coriolis, and transport acceleration, respectively. To obtain the associated scalar equations, it is necessary to define several coordinate systems and establish angular relationships describing the position and the motion of one system with respect to another.

The final equations set, usually adopted to analyze the dynamical behavior of a rigid body and completed by the variable mass system condition,[3] is able to describe the motion of a SSTO hypersonic space vehicle over a spherical and rotating Earth with no wind in the atmosphere:

$$\dot{V} = \frac{T\cos\varepsilon - D}{m} - g\sin\gamma + \omega^2 \cdot (R+h)\cos\lambda \cdot (\cos\lambda\sin\gamma - \sin\lambda\cos\gamma\sin\chi)$$

$$\dot{\chi} = \frac{(T\sin\varepsilon + L)\sin\mu}{mV\cos\gamma} - \cos\gamma\cos\chi\tan\lambda\frac{V}{R+h} + 2\omega\cdot(\cos\lambda\tan\gamma\sin\chi - \sin\lambda) - \omega^2\frac{R+h}{V\cos\gamma}\cos\lambda\sin\lambda\cos\chi$$

$$\dot{\gamma} = \frac{(T\sin\varepsilon + L)\cos\mu}{mV} - \left(\frac{g}{V} - \frac{V}{R+h}\right)\cos\gamma + 2\omega\cos\lambda\cos\chi + \omega^2\frac{R+h}{V}\cos\lambda\cdot(\sin\lambda\sin\gamma\sin\chi + \cos\lambda\cos\gamma)$$

$$\dot{\theta} = \cos\gamma\cos\chi\frac{V}{(R+h)\cos\lambda}, \qquad \dot{\lambda} = \cos\gamma\sin\chi\frac{V}{(R+h)}$$

$$\dot{h} = V\sin\gamma, \qquad \dot{m} = -\frac{T}{g_0 I_{\mathrm{sp}}} \quad (2)$$

This system of seven first-order differential equations, nonlinear and with nonconstant coefficients, denotes the instantaneous trim and position variations, as well as the mass losses of the whole space transport system. The dynamical system evolution is managed by means of the following meaningful parameters that have been adopted as control variables: angle of attack α, thrust angle ε, power setting δ, and bank angle μ.

Because the vehicle is requested to perform vertical liftoff by means of a full-rocket propulsion system, a shorter equation set has been employed to describe the first instants of the launch. (The equation system cannot accept $\gamma = 90$ deg.) In particular, a few seconds after the vertical launch, a path inclination angle of 89 deg, has been instantaneously adopted, without any loss of calculation accuracy:

$$\dot{V} = (T\cos\varepsilon - D)/m - g, \qquad \dot{\chi} = 0, \qquad \dot{\gamma} = 0$$

$$\dot{\theta} = 0, \qquad \dot{\lambda} = 0, \qquad \dot{h} = V, \qquad \dot{m} = -T/g_0 I_{\mathrm{sp}} \quad (3)$$

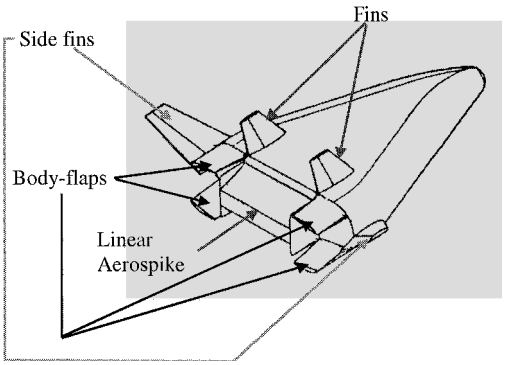

Fig. 1 Lifting-body concept vehicle.

Both the systems have been integrated by means of the RKSUITE software,[4] a suite of codes based on Runge–Kutta methods for the numerical solution of the initial values problems.

Gravitational and Atmospheric Model

Because the latitude variations and the uneven Earth's mass distribution have negligible effects on the acceleration of gravity, the gravitational field is assumed to be only function of the altitude, according to the inverse square law:

$$g(h) = g_0 \cdot [R/(R+h)]^2 \quad (4)$$

The atmospheric model follows the "US Standard Atmosphere 1962,"[5] including temperature profiles linearly dependent on the altitude.

Vehicle Configuration

The preliminary vehicle design, which originated from the reference scenario of an ESA's study, is a lifting-body concept vehicle (Fig. 1) performing vertical takeoff and horizontal landing and powered by a full-rocket propulsion system. Such a model has been adopted in accordance with the widely accepted requirements in terms of fully reusable vehicles, which means new space launchers' technical feasibility for the year 2005 and competitiveness with regards to launch costs.

Shape and size of the vehicle as well as the integrated propulsion system and weight distribution make reference to a complete data set originating from Alenia Aerospace and considering a fuselage length of 34 m, a total width of around 32 m, and a wing reference area of 500 m^2. The estimated gross liftoff weight (GLOW) is around 450,000 kg, whereas the operating empty weight, including structures, propulsion system, and thermal protections, is only 10% GLOW. The trim/maneuver capability on the pitch control is ensured by the thrust vectoring and the body-flap deflection, whereas the roll and the yaw control are respectively provided by the elevons, located on the side fins, and the rudders, located on the vertical tails.

The propulsion system includes seven linear aerospike rocket engines, which are able to guarantee optimal working conditions for the whole ascent. With respect to the conventional bell nozzle, the aerospike nozzle performs the gas expansion on its external surface, allowing the jet to expand efficiently at any altitude, thus providing higher mean specific impulse. Furthermore, the aerospike nozzle is shorter and lighter than the bell nozzle, and its shape can be positively integrated into the vehicle structure so that a lower aerodynamic drag and a better distribution of the thrust loads can be obtained. Finally the possibility to arrange seven rocket engines in a side-by-side configuration allows the thrust vectoring system to perform flight maneuvers easily.

Aerodynamic and Propulsive Model

The aerodynamic performances have been directly generated via a computational fluid dynamics Navier–Stokes code. The aerodynamic coefficients (C_L, C_D, and C_{MA}) have been tabulated in database form as functions of angle of attack, Mach number, and body-flap deflection angle and have been linearly interpolated in the program code.

The powerplant model adopted for the SSTO vertical liftoff vehicle is based on the innovative linear aerospike rocket engines and has been sized to provide a thrust/liftoff weight ratio $T/W = 1.4$, according to the safety specifications adopted in the ESA's study. This assumption can avoid the falling down of the launcher, in case one of the seven engine module should become not operating anymore; in such a case, even if the corresponding module on the opposite side of the aerospike engine should be turned off, the $T/W = 1$ can be guaranteed anyway. The aerospike engine configuration does not allow the thrust gimbals (see http//www.boeing.com/space/rdyne/x33/aerospik/aerospik.htm), but the pitch control during the whole ascent trajectory is performed by employing the thrust throttling in differential mode. On the basis of the vehicle configuration, it is realistic to assume the propulsion system able to provide: 1) axial thrust linearly depending on mean power setting and atmospheric pressure $T_X = T_X\ (P, \delta)$; 2) normal thrust linearly depending on atmospheric pressure and differential power setting $T_Z = T_Z\ (P, \tau)$, where the differential power setting τ is limited up to 30% of the mean power setting; and 3) pitch moment as a function of axial thrust, differential power setting, and c.g. position $M_P = M_P\ (T_X, \tau, X_{CG})$. The c.g. is assumed to linearly move along the longitudinal axis according to the vehicle mass variation. Because the thrust angle can be easily expressed in the form

$$\varepsilon = \tan^{-1}(T_Z/T_X) + \alpha \tag{5}$$

both the mean power setting δ and the differential power setting τ can be adopted in Eq. (2) as control variables for the ascent simulation as well as the angle of attack α, the body-flap deflection δ_f, and the bank angle μ.

Trajectory Optimization Problem

The investigation of optimal ascent trajectories for hypersonic space vehicles generally consists in a typical trajectory optimization problem,[6–8] where different sequential phases can be identified. By defining t the independent variable, the system is dynamically described during each trajectory phase by n_y states variables $y(t)$ and n_u control variables $u(t)$ and sometimes by n_p parameters, which are not depending on t.

The dynamical behavior of the system is usually defined by a set of ordinary differential equations, called *state equations* or *system equations*, written in explicit form:

$$\dot{y} = f[y(t), u(t), t] \tag{6}$$

which have to satisfy the following boundary conditions at the beginning and at the end of each phase:

$$F_l \le F[y(t), u(t), t] \le F_u \tag{7}$$

namely for $t = t_0$ and t_f. Moreover, the system solutions have to satisfy, in the following form, some definite path constraints

$$G_l \le G[y(t), u(t), t] \le G_u \tag{8}$$

as well as specific bounds on both the state and control variables

$$y_l \le y(t) \le y_u \tag{9}$$

$$u_l \le u(t) \le u_u \tag{10}$$

An equality constraint can be given in the same way, by simply imposing the upper bound to be equal to the lower one, i.e., $G_l = G_u$. The optimal control problem consists in determining the control variables vector able to minimize the objective function:

$$J = \Phi[y(t), t] \tag{11}$$

when $t \in [t_0, t_f]$ for each phase. By always taking into account that the larger the number of variables is the more complex is the objective function topology, the number of control parameters has to be reduced as much as possible in order to obtain an efficient optimization process.

Mission Description and Path Constraints

The simulation and optimization procedures have been applied to the ascent trajectory of a lifting-body full-rocket SSTO vehicle from the launch to the insertion into a Hohmann Transfer (H.T.) orbit.[9] During the optimization process, the maximum payload to GLOW ratio has been adopted as an objective function, the payload including all of the propellant mass losses as a result of the impulses of velocity required to accomplish the H.T. as well as the propellant mass contribution for deorbiting and beginning of the reentry phase. The fully reusable launcher has been designed to perform vertical liftoff, place the greatest possible payload into a 400-km orbit (where typically the ISS is going to be located), and return to the Earth along a reentry path trajectory by performing horizontal landing on a conventional tricycle landing gear.

Obviously the fulfillment to mission requirements cannot be limited to simply carry on such a payload at a specific altitude, but also consists in carefully complying with some constraint conditions, concerning both the ascent path trajectory and the correct injection into orbit. Upper limits on the dynamic pressure as well as on axial and normal acceleration have been taken into account to limit aerodynamic and mechanical loads on the vehicle structure for the entire mission. In particular, the admissible dynamic pressure is bounded to 40 kPa, and the axial and normal acceleration must not exceed 30 and 15 m/s^2, respectively.

Further constraint conditions, called *injection conditions*, have to be respected to enable a suitable orbit insertion: when entering into the elliptical transfer orbit, the path angle must be $\gamma = 0$ deg, and the spaceplane must have an orbital velocity only depending on the injection altitude and the major axis of the destination orbit. The spacecraft velocity value must satisfy the following relationship, directly originating from the energy equation:

$$V_{\text{orb}}^2 = GM \cdot [2/(R + h) - 1/a] \tag{12}$$

where V_{orb} is not the aircraft velocity with respect to the Earth, but it is the absolute inertial velocity referred to a nonrotating coordinate system centered in the center of the Earth and expressed by the following vectorial equation:

$$\boldsymbol{V}_{\text{orb}} = \boldsymbol{V} + \boldsymbol{\omega}_e \times \boldsymbol{r} \tag{13}$$

Besides, on the basis of geometrical relationships belonging to the spherical trigonometry field, a further injection condition relates the flight path direction to the latitude of the injection point and to the inclination of the final orbit according to the following relationship:

$$\sin\left(\chi + \frac{\pi}{2}\right) = \frac{\cos(i)}{\cos(\lambda)} \tag{14}$$

where, as just discussed, the angle χ is the absolute path direction, measured in a clockwise direction from east onward. Matching the injection conditions allows the spaceplane to avoid subsequent and costly correction maneuvers that are very difficult to execute in low Earth orbit (LEO) because of the quite high orbital velocity.

Preliminary Analysis and Control Laws

Taking into account the optimization requirements, a preliminary simulation analysis has been conducted to find the meaningful characteristics of the ascent flight path and therefore appropriately assign the maneuver control laws while minimizing the control parameters. The availability of a thorough aerodynamic data set and an accurate powerplant model has allowed the performance of a more realistic trajectory simulation analysis, where a further static trim condition on the pitch equilibrium for the whole ascent trajectory has been adopted by imposing the equality of pitch moments originating from the aerodynamic actions and the propulsive system

$$|M_P + M_A| \le \kappa \cong 0 \tag{15}$$

The first simulation results have confirmed the assumption that the inertial moments can be surely neglected with respect to the external moments (Fig. 2). The trim/maneuver capability on the pitch control is then ensured at each flight instant by a repetitive variation of the

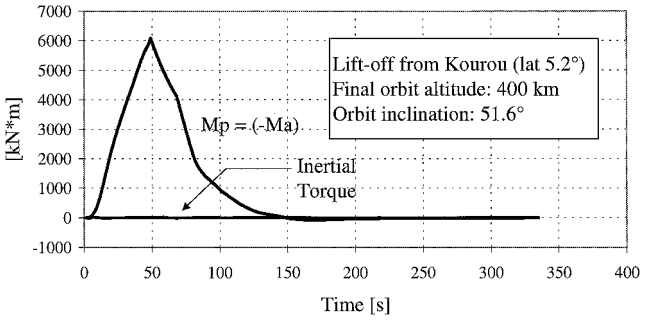

Fig. 2 External moments: Ma, aerodynamic moment, and Mp, propulsion moment.

thrust vectoring (via differential power setting control τ) and the body-flap deflection δ_f, according to the following relationships:

$$\Delta\tau = C_{\text{rm}} \cdot P\tau \qquad (0 \le C_{\text{rm}} \le 1)$$

$$\Delta\delta_f = (1 - C_{\text{rm}}) \cdot P\delta_f \qquad (0 \le C_{\text{rm}} \le 1)$$

where $P\tau$ and $P\delta_f$ are some constant parameters evaluated to be congruent with the variation field of τ and δ_f.

The preliminary analysis has shown the following:

1) The maximum payload is obtained by using the maximum available thrust, namely the maximum power setting values, according to the constraints on the axial acceleration and the dynamic pressure.

2) The velocity roll control law can be neglected during the whole ascent trajectory because the freedom of choosing the launch direction at the vertical liftoff enables the path direction at the end of the climb to be aligned to the destination orbit inclination. Thus $\mu = 0$ can be adopted at all times.

3) The static pitch trim provides the same results of a fully dynamic pitch trim, but reduces both problem complexity and computation time.

4) The maximum peaks of dynamic pressure and aerodynamic actions are reached in the transonic region (50–80 s after launch at an altitude of about 10 km), where also the differential power setting and the body-flap deflection achieve their maximum value during the flight path.

5) Because the angle-of-attack control law cannot be directly assigned as function of time $\alpha = \alpha(t)$, a new strategy has been needed to find the good starting point set of parameters in order to make easier the path trajectory control, reduce flight path angle oscillations in the central phase of the ascent, and be sure that velocity pitch will be very close to 0 deg when entering into the LEO outside the atmosphere.

Good Starting Point Methodology

One of the limits of direct gradient optimization methods is that optimal results are strongly influenced by the definition of a starting point set of parameters, namely, the set of control variables adopted as input for the optimization process drives the code toward a minimum, which often is a local minimum. Therefore, a new calculation routine has been implemented into the original simulation and optimization code in order to rapidly define a suitable set of parameters for the optimal starting conditions, the so-called good starting point, that is desirable for obtaining the correct result or, at least, a good local minimum of the objective function.

The investigation of optimal ascent trajectories for fully rocket propelled space transportation systems reveals great difficulties in the assignment of the initial guess at the angle-of-attack control law. This problem has been solved in our case by analyzing the third equation in Eq. (2), where the path inclination rate is expressed as a function of the following parameters:

$$\dot{\gamma} = \dot{\gamma}[T(\delta), \varepsilon(\alpha, \tau), L(\alpha, \delta_f), \mu] \qquad (16)$$

As just mentioned, the power setting δ has been assigned to obtain the maximum available thrust, and the velocity roll control μ has been neglected, whereas differential power setting τ and body-flap deflection δ_f are univocally determined by imposing static trim conditions on the pitch control. Therefore the path inclination rate can be assumed to be only a function of the angle of attack:

$$\dot{\gamma} = \dot{\gamma}(\alpha) \qquad (17)$$

This assumption allows the velocity pitch variation to be smoothed directly along the ascent trajectory because the simulation routine enables the step-by-step verification for each value of angle of attack, the instantaneous equivalence of the path inclination rate as resulting from the differential equation system, and a path angular velocity value imposed by a simple law $\dot{\gamma} = \dot{\gamma}(\gamma)$, able to satisfy the requirements at liftoff ($\gamma = 90$ deg) and at the injection into orbit ($\gamma = 0$ deg; $\dot{\gamma} = 0$ deg/s). The adopted procedure is able to control better the rotational dynamics when the path angular control law is provided in a spline variation form and enables the input variables to be more easily reset when a sensitivity analysis on different mission requirements is required to be performed.

Optimal Ascent Trajectory

On the basis of the preliminary analysis results concerning the ascent simulation and by applying the good starting point methodology just illustrated, the optimization process to define the optimal ascent trajectory ensuring the greatest payload/GLOW ratio has been finally run.

Before presenting the results and the control laws able to perform the optimal ascent trajectory, a new optimization routine, called multistep strategy (MSS) and created by the authors to more efficiently reach the minimum values of topologically complicated objective functions, is described. Moreover, a sensitivity analysis has been conducted to better appreciate the trajectory variations related to different mission requirements, and a specific optimization case has been addressed to evaluate the capability of aerodynamic and thrust vectoring trim conditions.

Multistep Strategy

The so-called MSS is a new routine, which has been implemented into the optimization code to attain more rapidly the minimum of the objective function during the optimization process. The single-step methodology, already adopted for optimizing the trajectories of airbreathing SSTO spaceplanes,[1] could not provide the same good results when applied to the ascent trajectory of a fully rocket vehicle because the obtainable gains in terms of payload/liftoff weight ratio are smaller than the improvements brought by optimization in the previous work. Instead of imposing a specific step for the whole optimization process, the MSS has allowed the optimization step to be increased or decreased differently according to the objective function topology, by continuously varying the increment value through repeated calls to the optimization routines.

The results of this new strategy, as shown in Fig. 3, have emphasized that a lower minimum of the objective function, resulting in a better payload to GLOW ratio, can be attained by repeatedly adopting a 2, 4, and 5% variation step on the control variables rather than a single 2% step. The MSS routine has obviously required a longer CPU time with respect to the single-step procedure, but the achieved gain in terms of optimal payload placed into orbit (3600 kg vs 3150 kg with the same starting point) deserves such an increase in computation time. Furthermore, referring to the same Fig. 3, the

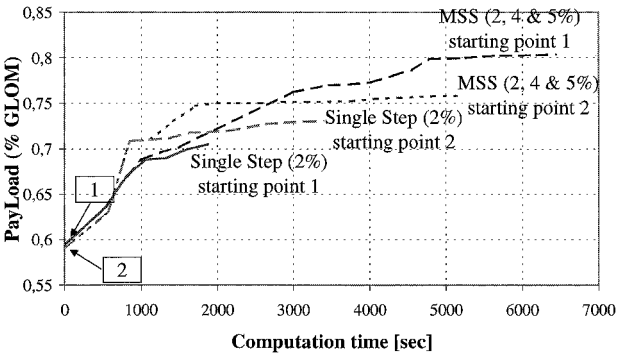

Fig. 3 Multistep strategy.

considerable influence of the starting set of parameters on the optimization results, as just mentioned, is clearly shown.

Sensitivity Analysis

A sensitivity analysis, by varying the final orbit inclination and altitude and the launch pad latitude, has been conducted to evaluate how different mission requirements or different starting conditions affect the optimal ascent trajectories in terms of final payload/liftoff weight ratio.

During the same analysis, the influence of specific control parameters and path constraints, like angle-of-attack control law and axial acceleration limit, has been investigated. In particular, three different orbit inclinations have been considered in order to estimate the payload possibilities, a nearly equatorial orbit ($i = 6$ deg), a nearly polar orbit ($i = 98$ deg), and the typical ISS orbit ($i = 51.6$ deg), with three different final altitudes (185, 250, 400 km) and two typical launch sites, Kourou (5.2° North) and Cape Canaveral (28.5° North).

Optimization Results

The main results of the analysis are presented in Figs. 4–12. A comparison between starting point and optimal ascent trajectories has revealed several differences in terms of guidance and control

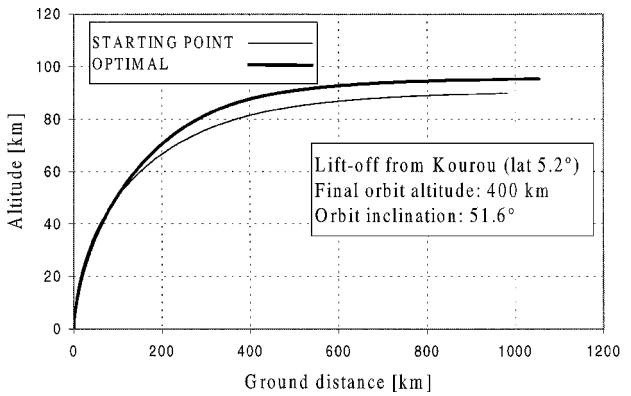

Fig. 4 Flight-path trajectory.

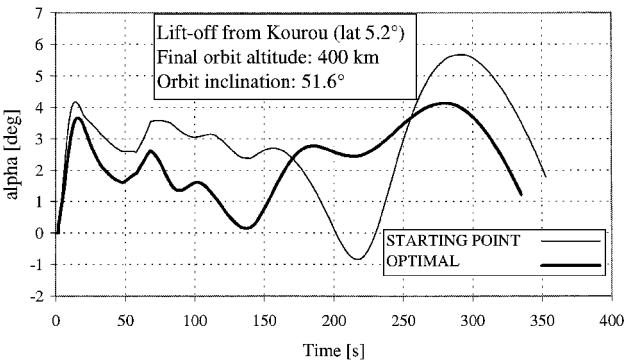

Fig. 5 Angle of attack.

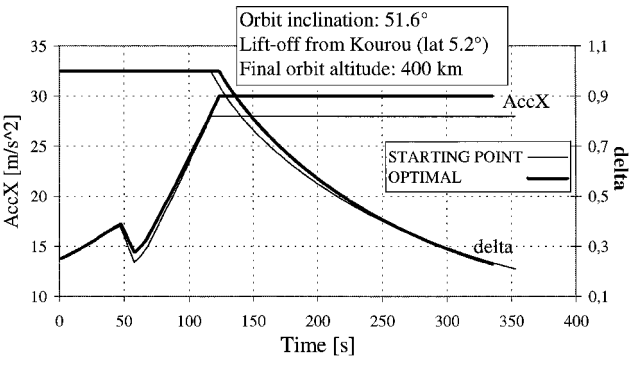

Fig. 6 Axial acceleration and power setting.

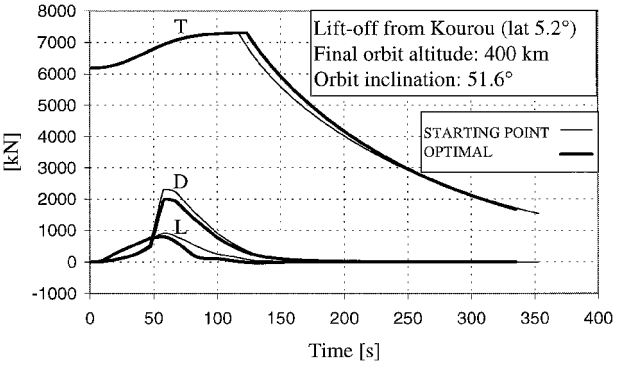

Fig. 7 Aerodynamic actions and available thrust: T, thrust; D, drag; and L, lift.

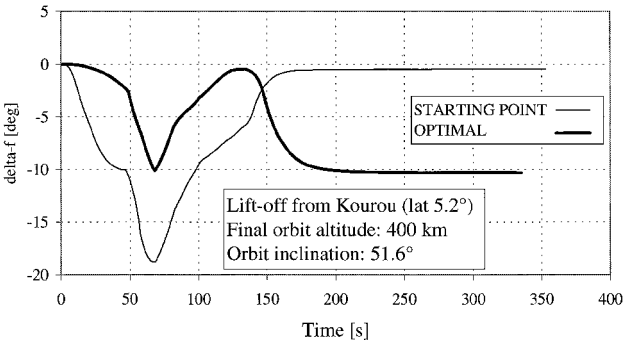

Fig. 8 Body-flap deflection.

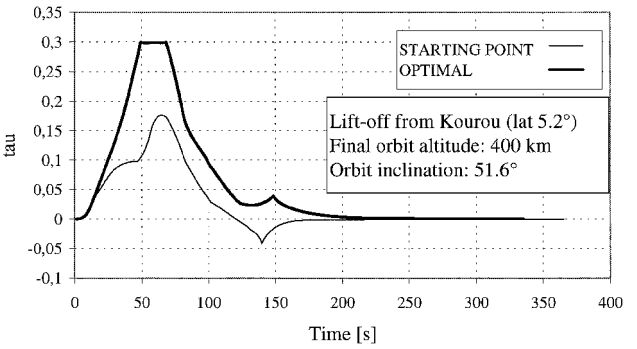

Fig. 9 Differential power setting.

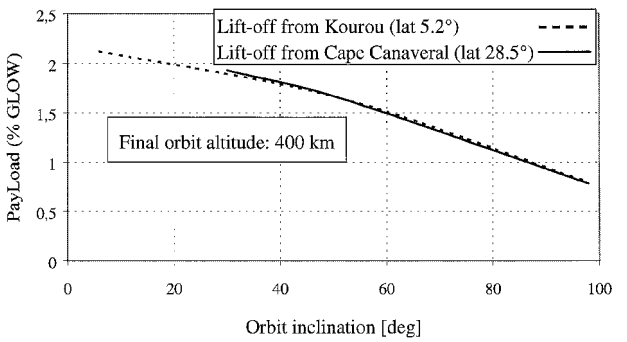

Fig. 10 Influence of orbit inclination and launch site latitude on the payload.

laws and flight-path parameters that can be shortly summarized as follows:

1) The optimized flight path is steeper at the beginning and smoother at the end of the climb with respect to the starting point trajectory (see Fig. 4), looking for the optimal compromise between gravity losses and aerodynamic drag. When considering a destination orbit of 400 km, the optimal parking altitude seems to be stabilized at about 90 km.

Table 1 Optimization results

Optimization results (empty weight: 10% of GLOW)	Payload % of GLOW
Orbit inclination 6 deg, altitude 400 km, liftoff from Kourou	1.90⇒ 2.11 (+0.21)[a]
Orbit inclination 51.6 deg, altitude 400 km, liftoff from Kourou	1.45⇒ 1.65 (+0.2)
Orbit inclination 98 deg, altitude 400 km, liftoff from Kourou	0.55⇒ 0.79 (+0.24)
Orbit inclination 30 deg, altitude 400 km, liftoff from Cape Canaveral	1.67⇒ 1.93 (+0.26)
Orbit inclination 51.6 deg, altitude 400 km, liftoff from Cape Canaveral	1.46⇒ 1.65 (+0.19)
Orbit inclination 98 deg, altitude 400 km, liftoff from Cape Canaveral	0.54⇒ 0.79 (+0.25)
Orbit inclination 98 deg, altitude 250 km, liftoff from Kourou	0.85⇒ 1.09 (+0.24)
Orbit inclination 98 deg, altitude 185 km, liftoff from Kourou	0.9⇒ 1.21 (+0.31)
Orbit inclination 6 deg, altitude 250 km, liftoff from Kourou	2.23⇒ 2.50 (+0.27)
Orbit inclination 6 deg, altitude 185 km, liftoff from Kourou	2.46⇒ 2.66 (+0.20)

[a]Arrows represent the improvement brought about by optimization.

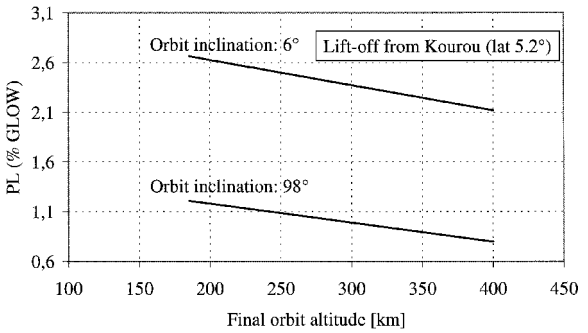

Fig. 11 Influence of final orbit altitude on the payload.

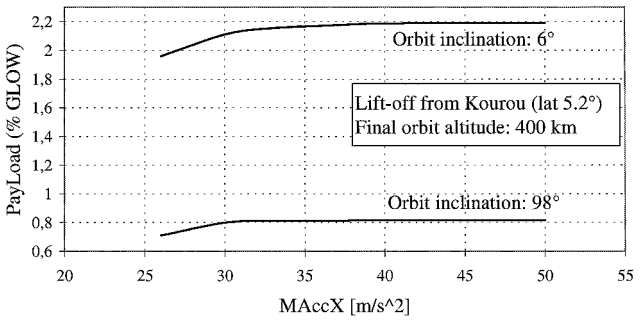

Fig. 12 Influence of axial acceleration limit on the payload.

2) During the whole optimal ascent trajectory, the angle-of-attack control law follows a more regular trend (variable in the range 0–4 deg), and so reducing aerodynamic losses and increasing thrust efficiency (Fig. 5).

3) The maximum normal acceleration is strongly reduced in the optimal ascent trajectory, whereas the axial acceleration always achieves the maximum permitted values to reduce the flight time to get the H.T. orbit.

4) In the same way the dynamic pressure as well as the peaks of aerodynamic actions appear to be reduced in the optimal flight path trajectory; therefore, the limit on the axial acceleration is the only one which occurs in reducing the available thrust (Fig. 6).

Very interesting results have been provided by the specific investigation addressed to evaluate the capability of aerodynamic and thrust vectoring trim conditions. Such an analysis has shown that the aerodynamic lift force plays a secondary role during the entire ascent trajectory so that the optimal ascent trajectory, ensuring the better payload/liftoff weight ratio in the trim conditions, should require the maximum thrust in accordance, with the path constraints (Fig. 7). Moreover, the thrust vector should be oriented along the speed direction as long as possible. Because of the simplified powerplant model, where efficiency losses caused by the thrust adjustments are not taken into account, the optimal trim conditions of the whole launch system are preferably guaranteed by thrust vectoring rather than by aerodynamic moments in order to minimize the additional aerodynamic drag caused by body-flap deflections (Figs. 8 and 9).

Optimization results concerning the sensitivity analysis on different mission requirements and starting conditions, as listed in Table 1, have demonstrated the following:

1) The two different launch site latitudes do not sensibly influence the optimal payload values, except for the 30-deg inclination orbit case, where an eastward launch from Cape Canaveral results to be more advantageous with respect to Kourou solution in terms of payload placed into orbit.

2) When considering a 400-km orbit, the maximum payload/liftoff weight ratio values obtained by the optimization process respectively correspond to 2.1% for the nearly equatorial orbit case and 0.8% for the nearly polar orbit case (Fig. 10).

3) The required propellant mass, and hence the optimal payload, are linearly dependent on the final orbit altitude for both the polar and the equatorial orbits, as shown in Fig. 11. Therefore, a maximum payload to takeoff weight ratio of 2.66% has been achieved starting from Kourou and getting an equatorial orbit at a final altitude of 185 km.

Furthermore, the influence of the axial acceleration limit on maximum payload placed into orbit has been specifically evaluated, and results have confirmed the 30 m/s^2 value as a suitable limit behind which the achievable gain in terms of payload becomes no longer interesting (Fig. 12).

Conclusions

A simulation and optimization methodology, applied to a new concept of vertical liftoff SSTO fully reusable launch vehicle, has been investigated in order to find optimal ascent trajectories according to typical mission profiles for serving a future manned space station. The adopted powerplant model, including seven linear aerospike rocket engines and operating with both linear and differential throttling modes, guarantees pitch moment control and optimal working conditions during the whole ascent trajectory.

A preliminary simulation analysis in static trim conditions has emphasized the possibility to neglect inertial effects on the pitch rotational equilibrium because they resulted extremely small if compared to aerodynamic and propulsive moments. This assumption has been successful to comply with the path constraints requirements and to provide the control adopted for the flight path simulation, whereas the suitable set of flight control parameters has been rapidly individuated through the application of the good starting point methodology.

During the optimization process, the application of the MSS to more accurately attain the minimum of the objective function has resulted in a 15% payload increase, the maximum axial acceleration being the only active constraint which reduces the available thrust. The subsequent sensitivity analysis on different mission requirements has clearly confirmed that the maximum payload placed into orbit is strongly influenced by the final altitude and inclination of the destination orbit. Accounting for the effects of Earth rotation and the propellant mass required by the reentry phase, the different optimal ascent trajectories have indicated typical values of final payload to gross liftoff weight ratio going from 0.8 to 2.1%, for

polar and equatorial orbit respectively at a final altitude of 400 km, whereas a maximum payload to takeoff weight ratio of 2.66% has been achieved starting from Kourou and getting an equatorial orbit at a final altitude of 185 km, as shown in Table 1.

The achieved results unequivocally provide useful indications for the next optimization step, which will consider the whole ascent and reentry mission. In particular a continuation of the present work should include the following topics: 1) investigation about how a nonlinear interpolation of the aerodynamic data set could affect the simulation and optimization precision; 2) estimation of the wind effects on the optimal climb path; 3) evaluation of the payload reduction when propellant reserves for an improved stability and dynamic control are considered; and 4) application of different optimization techniques, e.g., a genetic algorithm, to be adopted in alternative or in combination to the gradient optimization method.

Acknowledgments

The authors would like to express their sincere appreciation to Guido Colasurdo, Energetic Department, Politecnico di Torino, for several interesting discussions concerning orbital trajectories of fully rocket launch vehicles and to Alenia Aerospazio S.p.A., which has provided the data set information about vehicle configuration and propulsion system.

References

[1]D'Angelo, S., and Di Bona, D., "Guidance and Control for the Optimal Climb Trajectory of a SSTO Spaceplane," International Astronautical Federation, Paper IAF-96-A.4.11, Oct. 1996.

[2]Miele, A., *Flight Mechanics 1—Theory of Flight Path*, Vol. 1, Addison Wesley Longman, Reading, MA, 1962, pp. 58–65.

[3]Chudej, K., and Bulirsch, R., "Numerical Solution of a Simultaneous Staging and Trajectory Optimization Problem of a Hypersonic Space Vehicle," AIAA Paper 93-5130, Dec. 1993.

[4]Brankin, R. W., Gladwell, I., and Shampine, L. F., "RKSUITE: a Suite of Runge–Kutta Codes for the Initial Value Problem for ODEs," Softreport 92-S1, Dept. of Mathematics, Southern Methodist Univ., Dallas, Texas, 1992.

[5]"US Standard Atmosphere 1962," U.S. Weather Bureau, NASA, and U.S. Air Force, 1962.

[6]Betts, J. T., "Survey of Numerical Methods for Trajectory Optimization," *Journal of Guidance, Control, and Dynamics*, Vol. 21, No. 2, 1998, pp. 193–207.

[7]Betts, J. T., and Cramer, E. J., "Application of Direct Transcription to Commercial Aircraft Trajectory Optimization," *Journal of Guidance, Control, and Dynamics*, Vol. 18, No. 1, 1995, pp. 151–159.

[8]Paus, M., and Well, K., "Optimal Ascent Guidance for a Hypersonic Vehicle," AIAA Paper 96-3901, July 1996.

[9]Cornelisse, J. W., Schoyer, H. F. R., and Wakker, K. F., *Rocket Propulsion and Spaceflight Dynamics*, Pitman, London, 1979, pp. 389–395.

J. A. Martin
Associate Editor